STEM CELLS AND DEVELOPMENT
Volume 23, Number 17, 2014

DOI: 10.1089/scd.2013.0563

Inhibition of TROY Promotes OPC Differentiation and Increases Therapeutic Efficacy of OPC Graft for Spinal Cord Injury

Liang Sun,[1] Shengliang Liu,[1] Qi Sun,[1] Zhuying Li,[2] Fengyan Xu,[1] Chunmei Hou,[1] Toshihide Harada,[3] Ming Chu,[4] Kun Xu,[4] Xiaoling Feng,[2] Yongshun Duan,[4] Yafang Zhang,[1] and Shuliang Wu[1]

Endogenous or graft-derived oligodendrocytes promote myelination and aid in the recovery from central nervous system (CNS) injury. Regulatory mechanisms underlying neural myelination and remyelination in response to injury, including spinal cord injury (SCI), are unclear. In the present study, we demonstrated that TROY serves as an important negative regulator of oligodendrocyte development and that TROY inhibition augments the repair potential of oligodendrocyte precursor cell (OPC) graft for SCI. TROY expression was detected by reverse transcriptase–polymerase chain reaction in OPCs as well as in differentiated premature and mature oligodendrocytes of postnatal mice. Pharmacological inhibition or RNAi-induced knockdown of TROY promotes OPC differentiation, whereas overexpression of TROY dampens oligodendrocyte maturation. Further, treatment of cocultures of DRG neurons and OPCs with TROY inhibitors promotes myelination and myelin-sheath-like structures. Mechanically, protein kinase C (PKC) signaling is involved in the regulation of the inhibitory effects of TROY. Moreover, in situ transplantation of OPCs with *TROY* knockdown leads to notable remyelination and neurological recovery in rats with SCI. Our results indicate that TROY negatively modulates remyelination in the CNS, and thus may be a suitable target for improving the therapeutic efficacy of cell transplantation for CNS injury.

Introduction

Oligodendrocyte precursor cells (OPCs), a distinct population of glial cells characterized by expression of nerve/glial antigen 2 (NG2) and platelet-derived growth factor receptor-α (PDGFRA), produce mature myelinating oligodendrocytes throughout life [1]. OPCs originate from neural stem cells and constitute ~5% of all cells in the adult brain [1,2]. OPCs are highly proliferative and migratory bipolar cells [3,4]. They differentiate into the $O4^+$ premyelinating oligodendrocytes, which further differentiate into mature myelinating oligodendrocytes, a process characterized by the emergence of the expression of myelin basic protein (MBP), proteolipid protein (PLP), or myelin-associated glycoprotein (MAG) [1,4]. Mature oligodendrocytes wrap around and myelinate axons, thereby supporting saltatory conduction across them [1,5].

Traumatic spinal cord injury (SCI) leads to long-term health, economic, and social consequences worldwide. Unfortunately, current therapies have relatively limited efficacy [6]. Apart from axonal injury and neuronal loss, another important pathological feature of SCI is failed remyelination, which disrupts impulse conduction across the remaining axons and affects post-SCI functional recovery. Failed remyelination in SCI is associated with failure of OPCs to differentiate into mature myelinating oligodendrocytes [7,8]. Therefore, strategies aimed at promoting differentiation and remyelination of host and grafted OPCs can improve motor functional recovery after SCI.

Previous studies have indicated that the development of oligodendrocytes is complicatedly controlled both intrinsically by transcription factors and chromatin remodeling [4,9], and extrinsically by neuronal and glial activity [10,11]. Moreover, many extracellular signaling molecules regulate the differentiation of OPCs by activating corresponding receptors on the cell surface [12–15]. In addition, a few intracellular signaling pathways, such as the RhoA-ROCK and protein kinase C (PKC) pathways, are implicated in the maturation of oligodendrocytes [16–21]. However, which extrinsic signal dominates and how the ligand-receptor

[1]Department of Anatomy, School of Basic Medical Sciences, Harbin Medical University, Harbin, China.
[2]The First Affiliated Hospital of Heilongjiang University of Chinese Medicine, Harbin, China.
[3]Faculty of Health and Welfare, Prefectural University of Hiroshima, Hiroshima, Japan.
[4]The First Affiliated Hospital of Harbin Medical University, Harbin, China.

signals are transmitted inside cell to trigger differentiation are yet to be determined.

TROY (also known as TAJ), classified as the tumor necrosis factor receptor superfamily member 19, is broadly expressed in the postnatal and adult central nervous system (CNS) [22–25]. As a component of the Nogo receptor complex, TROY mediates myelin-derived inhibitory ligands [Nogo 66, MAG, and oligodendrocyte-myelin glycoprotein (OMG)] and induces axon outgrowth inhibition in the adult mammalian CNS [26,27]. Of note, myelin impairs CNS remyelination by repressing OPC differentiation [19,28]. A major unresolved issue is whether TROY is expressed in the oligodendrocyte lineage. Further, whether and how TROY is involved in the regulation of oligodendrocyte maturation is also unclear. In the present study, we explored the role of TROY in oligodendrocyte differentiation and remyelination after SCI. Our long-term objectives were to identify novel targets for remyelination therapies.

Materials and Methods

Primary cell culture

All procedures involving animals were conducted in accordance with the guidelines of the Harbin Medical University and were approved by the local Institutional Committee for Animal Care. Dorsal root ganglions (DRGs) were dissected from 4-week-postnatal C57BL/6 mice (Institute of Model Animal, Nanjing, China) and were dissociated using 0.2% collagenase (Sigma-Aldrich) and 0.1% trypsin (Sigma-Aldrich) at 37°C for 40 min. Dissociated cells were plated on coverslips coated with poly-D-lysine (10 mg/mL; Invitrogen) at a density of 5×10^5 cells/mL. Cells were grown for 2 weeks in Neurobasal medium (Invitrogen) supplemented with 10% fetal bovine serum (FBS; Invitrogen) and 1% penicillin/streptomycin (Sigma-Aldrich). To remove contaminating fibroblasts and glial cells, cultures were pulsed twice with fluorodeoxyuridine (15 μM) from day 2 to 6 and from day 8 to 10.

OPCs were obtained using a standard protocol with minor modifications [29]. In brief, the cerebral cortices from postnatal 0–2-day (P0-2) C57BL/6 mice or enhanced green fluorescence protein (EGFP)–transgenic mice [C57BL/6-Tg (CAG-EGFP) 1Osb/J; Institute of Model Animal, Nanjing, China] were dissected and the meninges were removed before mechanical and enzymatic dissociation. Dissociated cells were cultured in poly-D-lysine-coated T75 tissue culture flasks in Dulbecco's modified Eagle's medium/F-12 (DMEM/F-12; Invitrogen) supplemented with 10% FBS and 1% penicillin/streptomycin. After 10–12 days, the flasks were shaken on an orbital shaker at 180 rpm for 30 min to remove neurons and astrocytes. Media were subsequently replaced, and the flasks were shaken overnight at 220 rpm. Media were collected and plated on noncoated bacteriologic plastic dishes for 20–30 min to eliminate contaminating microglia. The final supernatant from cultures contained ~85%–90% OPCs. OPCs were cultured in DMEM/F-12 supplemented with 10% FBS and 1% penicillin/streptomycin for 1 week. With the purity of NG2-positive OPCs determined, OPCs ($NG2^+$) were differentiated into premature oligodendrocyte ($O4^+$) and consecutively mature oligodendrocyte (MBP^+) in differentiation medium comprising DMEM/F-12 supplemented with triiodo-L-thyronine (T3; 1.0 mM; Sigma-Aldrich) and 1% penicillin/streptomycin. The purity and differentiation of each culture were monitored by phase-contrast microscopy (AX70; Olympus Optical) and immunocytochemistry. Only those cultures exhibiting >94% purity were employed.

Experimental design

To determine the expression of TROY in the oligodendrocyte lineage, purified $NG2^+$, $O4^+$, or MBP^+ cell cultures were subjected to reverse transcriptase–polymerase chain reaction (RT-PCR) analysis. To test the involvement of TROY in OPC differentiation, purified OPCs were plated onto poly-D-lysine-coated glass coverslips, cultured for 4–6 h in DMEM/F-12 supplemented with 10% FBS and 1% penicillin/streptomycin, and then transferred to DMEM/F-12 supplemented with soluble human TROY (TROY-Fc; 10 μg/mL; Sigma-Aldrich) which serves as the antagonist of TROY [26] or control Fc (10 μg/mL; Sigma-Aldrich) for differentiation assay. For dose-response assay, primary OPCs were cultured in DMEM/F-12 supplemented with TROY-Fc at gradient concentration (0, 1, 2, 4, 6, 8, 10, 12, 16, and 20 μg/mL) before differentiation assay. For further study, cells were grown in the differentiation medium and instantly treated with *TROY* RNA interference (RNAi) lentiviral vector, *TROY* lentiviral expression vector, or *TROY* lentiviral expression vector plus a PKC inhibitor. After 72 h, *TROY* RNAi lentiviral vector– and *TROY* lentiviral expression vector–treated cultures were subjected to immunocytochemical staining for O4 or western blot analysis for c-Jun N-terminal Kinase (c-JNK), PKC, or phosphorylated protein kinase C (p-PKC). Cultures treated with blank lentiviral vector (BLV), BLV plus PKC inhibitor, *TROY* lentiviral expression vector, or *TROY* lentiviral expression vector plus PKC inhibitor for 7 days were subjected to western blot analyses to determine the expression levels of MBP. To study in vitro myelination by OPCs in cocultures of OPCs and DRG neurons, $NG2^+$ OPCs were added to DRG neuron drop cultures in the presence or absence of 10 μg/mL TROY-Fc. The culture medium (neurobasal medium complemented with 1% penicillin/streptomycin) was exchanged, and fresh TROY-Fc was added to the cultures every 3 days. To identify differences in myelination, 2-week-old cocultures were analyzed by immunocytochemistry. Myelination was identified as regions of colocalization between MBP-positive oligodendrocyte processes and β-tubulin-III-positive neurites and quantified as reported previously [30]. To identify the effects of TROY on the repair potential of graft-derived oligodendrocytes following SCI, purified green fluorescence protein (GFP)–positive OPCs treated with *TROY*-RNAi for 72 h were transplanted in rats with SCI, followed by histological, behavioral, and electrophysiological assays.

Immunocytochemistry

Samples were fixed in 4% paraformaldehyde in PBS (pH 7.4) for 20 min, permeabilized in 0.5% Triton X-100 in PBS (pH 7.4) for 15 min, and blocked with 3% bovine serum albumin (BSA; Invitrogen) in PBS (pH 7.4) for 20 min. Subsequently, samples were incubated with anti-NG2 (rabbit IgG; 1:200; Cell Signaling Technology, Inc.), anti-O4 (rabbit IgG; 1:200; Abcam), anti-MBP (mouse IgG; 1:200; Cell Signaling Technology), or anti-β-tubulin III (rabbit

IgG; 1:200; Abcam) primary antibodies in 1% BSA overnight at 4°C and incubated for 1 h with secondary antibody (goat anti-rabbit IgG-Alexa Fluor 594, goat anti-rabbit IgG-Alexa Fluor 488, or goat anti-mouse IgG-Alexa Fluor 594; 1:5,000; Molecular Probes, Invitrogen) for 20 min at room temperature in the dark. Nuclei were stained with 4′,6′-diamidino-2-phenylindole (DAPI; 1:500; Sigma-Aldrich). Samples were analyzed by fluorescence microscopy (BX51; Olympus).

Reverse transcriptase–polymerase chain reaction

Total RNA was harvested from cell samples using RNeasy Mini Kit (Qiagen) according to the manufacturer's instructions. Reverse transcription of 500 ng of RNA (each sample) was performed with first-strand cDNA synthesis kit (Roche Applied Science) according to the manufacturer's protocol. RT-PCR was used to quantify *TROY* mRNA levels in primary cultured OPCs, using the forward primer (5′-GAATCCAAGCTTGCACTCAAGGTCCTACCTCTA CAC-3′) and reverse primer (5′-ATATATGGGCCCTCAG GCATCCTGGAAG-3′). Primers were designed using Primer Express v3.0 (Applied Biosystems). Data were normalized to β-actin levels.

Infection by lentiviral vectors

Four to 6 h after purified $NG2^+$ OPCs were plated on poly-lysine-coated coverslips, cells were infected with RNAi lentiviral vectors for *TROY*, expression lentiviral vectors for *TROY*, or BLVs. All lentiviral vectors were GFP labeled. A multiplicity of infection of five was used in the presence of polybrene (D-Biopharm Biotech Co. Ltd) according to the manufacturer's instructions. After 72 h, the efficacy of lentiviral vector infection was quantified using an Olympus BX51 fluorescent microscope. To determine the knockdown or expression efficiency of the targeted genes, RT-PCR analyses were performed to detect *TROY* mRNA levels. OPC differentiation was assessed by immunocytochemistry 72 h after lentiviral vector infection as outlined earlier. To quantify the effects of RNAi on differentiation, only GFP-expressing oligodendrocytes were counted.

Pharmacological inhibition of PKC

To examine whether PKC transduction is implicated in TROY-mediated OPC differentiation arrest, a pharmacological inhibitor was used to block PKC signaling. The selective PKC inhibitor bisindolylmaleimide (BIM; Sigma-Aldrich) solubilized in dimethyl sulfoxide (DMSO; Invitrogen) was added to the culture medium immediately after cells were seeded for blank lentiviral expression vector or *TROY* lentiviral expression vector infection. Total cellular protein was extracted from OPCs differentiated for 7 days and the expression of MBP was evaluated by western blot analysis.

Western blot analysis

Cell samples were lysed in a buffer containing 10 mM Tris (pH 7.4), 100 mM NaCl, 1 mM EDTA, 1 mM EGTA, 1 mM NaF, 20 mM $Na_4P_2O_7$, 2 mM Na_3VO_4, 0.1% SDS, 0.5% sodium deoxycholate, 1% Triton-X 100, 10% glycerol, 1 mM PMSF, 60 mg/mL aprotinin, 10 mg/mL leupeptin, and 1 mg/mL pepstatin. After high-speed centrifugation, protein concentration was measured using bicinchoninic acid (BCA) protein assay (Sigma-Aldrich) and 15 mg was loaded on SDS-PAGE for separation. Western blot was conducted using a Multiphor II Electrophoresis System (Bio-Rad Laboratories, Inc.) at 200 mA for 1 h and 30 min. After blocking with 5% BSA in TBS-T (0.1% Triton × 100 in TBS) for 1 h at room temperature, the blots were incubated with anti-c-JNK (rabbit IgG; 1:1,000; Proteintech Group, Inc.), anti-PKC-α (rabbit IgG; 1:1,000; Santa Cruz Biotechnology, Inc.), anti-p-PKC-α (rabbit IgG; 1:1,000; Santa Cruz Biotechnology, Inc.), anti-MBP (mouse IgG; 1:1,000; Cell Signaling Technology), or anti-β-actin (rabbit IgG; 1:1,000; Cell Signaling Technology) primary antibodies overnight at 4°C. Following incubation with horseradish-peroxidase-conjugated secondary antibody (goat anti-rabbit IgG or goat anti-mouse IgG; 1:5,000; Molecular Probes, Invitrogen) for 1 h, the immunoreactive bands were detected by the enhanced chemiluminescence western blotting detection reagent (GE Health Care Bio-Sciences) on a film. Densitometric analysis was performed using Image Pro Plus 6.0 software.

SCI induction and cell transplantation

Female Sprague-Dawley (SD) rats (Institute of Model Animal, Nanjing, China) were randomly assigned to *TROY*-knockdown OPC (TKD-OPC) group, BLV-treated OPC (BLV-OPC) group, sham treatment group, and sham surgery group. Moderate SCI was induced and identical postoperative animal care was performed on all animals, as reported previously with slight modifications [31]. In brief, animals were anesthetized by intraperitoneal (i.p.) injection of 4% chloral hydrate (0.5 mL/100 g). Back skin was shaved and scrubbed with ethanol. A dorsal laminectomy was performed at thoracic segment (T) 9 or T10 to expose the spinal cord without disrupting the dura. Using the Ohio State University contusion device, an impact probe of 10 g in weight and 2.5 mm in diameter was lowered onto the exposed dural surface at a height of 12.5 mm. To prevent bleeding, gelfoam was placed on the dural surface and successively muscle and skin were closed in layers. Animals were kept in heating chambers (37°C) overnight. Penicillin (3,000 U/100 g) was administered for 7 days to prevent infection. Manual expression of urinary bladder was performed twice daily until voluntary bladder emptying recovered. For the sham surgery group, the animals were subjected to a T10 laminectomy without impact injury.

Seven days following SCI, animals were re-anesthetized as described previously, followed by the re-exposure of the laminectomy site. Successively, 5 μL of GFP^+ OPCs (1×10^5/μL) in sterile PBS (PH 7.4) was injected in situ at the epicenter of the injury. The injected cells were allowed to settle for at least 5 min before the needle was retracted. The muscle and skin were subsequently sutured and closed in layers. Appropriate postoperative treatment was performed on experimental animals, as described previously. Rats in the TKD-OPC group received *TROY*-RNAi-treated GFP^+ OPC graft, whereas those in the BLV-OPC group received BLV-treated GFP^+ OPC graft. Rats in sham treatment group underwent equal volume of sterile PBS in situ injection

and rats in sham operation group received no injection. To suppress host immunological rejection, cyclosporine A (10 mg/kg; Sigma-Aldrich) was injected i.p. to all groups for 7 days after grafting.

Histological analyses

To define the anatomical location of the lesions, injured spinal cords were subjected to hematoxylin-eosin (HE) staining. To measure the demyelination and remyelination of the lesion sites of spinal cord, Luxol fast blue staining was performed in accordance with the standard protocol. To verify cell graft survival, integration, and differentiation in the host tissue, immunohistochemistry was conducted. In brief, frozen sections of the spinal cord were blocked using 5% BSA and 0.25% Triton X-100 for 1 h, incubated overnight at 4°C with anti-MBP (mouse IgG; 1:200; Cell Signaling Technology), or GFP primary antibodies (rabbit IgG; 1:200; Proteintech Group). All antibodies were diluted with Tris-buffered saline supplemented with 0.5% Tween 20 (TBST). After incubation with secondary antibody (goat anti-mouse IgG-Alexa Fluor 594 or goat anti-rabbit IgG-Alexa Fluor 488; 1:5,000; Molecular Probes, Invitrogen) for 20 min and counterstaining with DAPI (1:500; Sigma-Aldrich) for 5 min at room temperature in the dark, sections were viewed using a fluorescence microscope (BX51; Olympus).

For the histological ultrastructural analyses, experimental animals of different groups were perfused with 2.5% gluteraldehyde in 0.1 M cacodylate buffer (pH 7.4). Spinal cords between 0.5 mm on either side of the epicenter of injury were excised and fixed in 2.5% gluteraldehyde in 0.1 M cacodylate buffer (pH 7.4), processed with 1% osmiumtetroxide/1.5% potassium ferrocyanide, and washed extensively. Having been stained in uranyl acetate, samples were then dehydrated and embedded in Epon 812 epoxy resin. Ultrathin sections (60 nm) were cut on a Leica Ultra-CUT (Ultra-Microtome, Leica Microsystems GmbH), mounted on 200-mesh copper grids, stained with uranyl acetate and lead citrate, and viewed under a transmission electron microscope (TEM; H-7650; Hitachi). Images were captured with a MegaView III CCD camera (Soft Imaging System).

Behavioral tests

For assessing motor function deficit and recovery, BBB assessment and inclined plane test were conducted. Animals were adapted to these tasks every second day starting from 1 week before surgery. These motor function tests were performed on days 1, 3, 7, 10, 14, 17, 21, 24, and 28 following SCI. BBB assessment trials were performed in accordance with the procedure described by Basso et al. [31]. In brief, this scale used for assessing hindlimb function includes evaluation standards ranging from a score of 0, indicating no spontaneous movement, to a maximum score of 21, with an increasing score indicating the use of individual joints, coordinated joint movement, coordinated limb movement, weight-bearing, and other functions. Two researchers ''blinded'' to rat treatment status performed 4-min tests on all animals. The inclined plane analysis was selected as another index of hindlimb strength. For this, rats were placed on a board so that their body axis was perpendicular to the axis of an inclined plane. The maximum angle at which a rat was able to maintain its position for at least 5 s constitutes the inclined plane score. All behavioral tests were recorded using a digital camera.

Electrophysiological evaluation

Motor-evoked potential (MEP) was examined using a custom demultiplexer (MEB-9402; Nihon Kohden) as described previously with slight modifications [32]. In brief, rats were randomly selected and injected with 4% chlorate hydrate (0.5 mL/100 g) and xylazine (1 mg/100 g). Ten square-wave stimuli with duration of 0.2 ms, a stimulus intensity of 0.4 mA, and an interstimulus interval of 1 Hz were transmitted through the occipitocervical area of the spinal cord and hindlimb by needle electrodes. The active electrode was placed in the muscle belly, whereas the reference electrode was placed near the distal tendon of the muscle in the hindlimb and the ground electrode was placed on the tail.

To assess the somatosensory evoked potential (SEP), rats were anesthetized 1 week before the injury, and their head was shaved and sterilized with 75% ethanol. Electrode pedestals were implanted into the skull as previously described [33]. A standard dental drill (Fine Science Tools) was used to drill 3 burr holes into the exposed part of the cranium at locations of the primary somatosensory cortex corresponding to the hindlimbs (2.8-mm lateral and 2.5-mm posterior to the bregma). The third hole drilled on the right frontal bone, 2 mm from the sagittal and coronal sutures, served as the intracranial reference. Transcranial screw electrodes (E363/20; Plastics One, Inc.) were secured into the holes so that they were in very light contact with the duramater, and they were mounted to electrode pedestals (MS363; Plastics, One Inc.) using dental cement. For SEP recordings, rats were anesthetized with 4% chlorate hydrate. Tibial nerves of hindlimbs were electrically stimulated with subcutaneous needle electrodes (Safelead F-E3-48; Grass-Technologies). For each session, both hindlimbs were stimulated in an alternating fashion and the corresponsive SEPs were recorded. Stimuli generated by a custom demultiplexer (Plastics One, Inc.) were delivered at 1 Hz so that each limb received a pulse with a frequency of 0.25 Hz, an intensity of 3 mA, and a pulse width of 200 ms. A subdermal electrode placed at the back of the neck served as a reference ground electrode. Signals of SEPs were processed with MATLAB 7.0 (MathWorks, Inc.).

For MEP and SEP, the onset latency was gauged as the time interval in millisecond between the stimulus and the onset of the first wave. Ten responses in each rat were averaged for the latency analysis. Electrophysiological evaluations were performed 1 and 4 weeks following SCI.

Statistical analyses

For all studies at least three independent experiments were performed. Data processing and statistical analyses were performed using Microsoft Excel and GraphPad Prism Software. Data are presented as the mean ± standard deviation (SD) or mean ± standard error of the mean (SEM). Student's *t*-test, one-way analysis of variance, or two-way analysis of variance followed by a Bonferroni's multiple-comparison *post hoc* test was used to determine differences between groups. A P-value of < 0.05 was considered statistically significant.

Results

TROY is expressed in oligodendrocyte lineage and involved in the negative regulation of OPC differentiation

Purified neonatal mice-derived OPCs exhibit bipolar shape and NG2-positive immunophenotype in proliferation medium containing FBS (Fig. 1A). TROY expression was verified using RT-PCR and western blot in neonatal C57BL/6 mice-derived $NG2^+$ OPCs and differentiated $O4^+$ and MBP^+ oligodendrocytes (Fig. 1B, C), indicative of the function TROY exerted on oligodendrocyte lineage. To test whether TROY is involved in the regulation of oligodendrocyte differentiation, purified OPCs were transferred to DEME/F-12 supplemented by only TROY-Fc (10 μg/mL), which contains the extracellular domain of TROY and serves as the competitive antagonist to block the TROY effect [26]. Similar to T3-induced oligodendrocyte development in vitro [30,34–36], ~80% of TROY-Fc-treated OPCs were differentiated into $O4^+$ premature oligodendrocytes with longer and more branched processes after a 14-day treatment ($F = 869.4$; TROY-Fc, $P > 0.05$ versus T3; $n = 10$ per group; Fig. 2A, B). In contrast, the $O4^+$ cells were below detectable limit in control Fc-treated cultures (Fig. 2A, B). When treatment was extended to 21 days, the majority of TROY-Fc-treated cells displayed myelin sheet structures and MBP-positive immunoreactivity, which was close to but not equivalent to oligodendrocyte maturation in presence of T3 ($F = 3{,}634$; TROY-Fc, $P < 0.05$ versus T3; $n = 10$ per group). However, MBP^+ cells were barely observed in control Fc-treated cultures (Fig. 2C, D). Further, as revealed by dose-response assay at day 14, TROY-Fc promoted oligodendrocyte differentiation in a concentration-dependent manner with a half-maximum effective concentration (EC_{50}) of 6 μg/mL (Fig. 2E). Over the period of observation, cells grown in DMEM/F-12 supplemented with control Fc exhibited OPC-specific bipolar morphology and $NG2^+$ immunostaining with no evidence of differentiation (Fig. 2F). These findings implicated that TROY was expressed in oligodendrocyte lineage in the negative regulation of OPC differentiation.

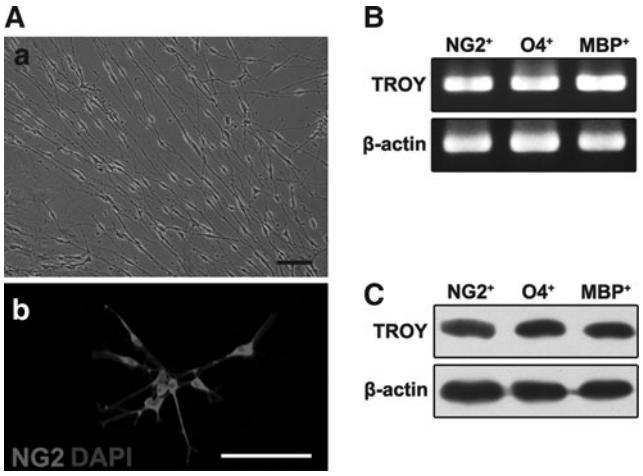

FIG. 1. TROY is expressed in oligodendrocyte lineage. **(A)** Purified OPCs cultured in proliferation medium containing 10% FBS. **(a)** Phase-contrast image of purified OPCs. **(b)** Immunofluorescence images of OPCs stained for NG2 and counterstained by DAPI. **(B)** Images of RT-PCR analysis exhibiting *TROY* mRNA expression in neonatal C57BL/6 mice-derived NG2-positive OPCs and differentiated O4-positive and MBP-positive oligodendrocytes. β-Actin expression was tested as an internal control. **(C)** Images of western blot analysis exhibiting TROY protein expression in neonatal C57BL/6 mice-derived NG2-positive OPCs and differentiated O4-positive and MBP-positive oligodendrocytes. β-Actin expression was tested as an internal control. Scale bar **(A)** = 100 μm. DAPI, 4′,6′-diamidino-2-phenylindole; FBS, fetal bovine serum; MBP, myelin basic protein; NG2, nerve/glial antigen 2; OPC, oligodendrocyte precursor cell; RT-PCR, reverse transcriptase–polymerase chain reaction.

TROY inhibition contributes to oligodendrocyte maturation and myelination

To further evaluate the effects of TROY on the differentiation of oligodendrocyte, purified OPCs were cultured in the presence of canonical oligodendrocyte development inducer T3. TROY was attenuated by RNAi. Purified NG2-positive OPC cultures were treated with *TROY*-RNAi for 72 h and the decrease of *TROY* transcription was verified by RT-PCR and western blot (Fig. 3A, B). Subsequently cells were stained for the canonical marker of premyelinating oligodendrocyte O4. Consistent with the findings of TROY-Fc treatment, *TROY* knockdown (TKD) increased O4-positive cells with branched and membranous processes ($F = 180.8$; TKD, $P < 0.001$ versus BLV; $n = 10$ per group; Fig. 3C, E), indicating enhanced oligodendrocyte maturation. Conversely, TROY overexpression (TOE) by lentiviral expression vector transduction for 72 h in OPCs, which was confirmed by RT-PCR (Fig. 3A, B), resulted in 50% decrease in premature oligodendrocytes in contrast to that by BLV transduction group ($F = 180.8$; TOE, $P < 0.001$ versus BLV; $n = 10$ per group; Fig. 3C, E). These data verified the promotion of oligodendrocyte differentiation by inhibition of TROY.

To further assess the effects of TROY on myelination in vitro, cocultures of OPCs and neurons were established. In accordance with previous data [30,37], cocultures of rodent primary oligodendrocytes and DRG neurons exhibited relatively poor myelination. Treatment of TROY-Fc for 2 weeks markedly stimulated myelination in these cultures (Fig. 3D, F). Through identification of the colocalization of MBP-positive oligodendrocyte processes and β-tubulin-III-positive neurites, TROY-Fc-treated cocultures were observed to develop myelin-sheath-like structure surrounding neuronal axons, which resembled the T3-induced myelination in vitro [30]. In comparison, the axons in cocultures treated with control Fc of equal volume remained poorly myelinated ($t = 19.10$; TROY-Fc, $P < 0.001$ versus control Fc; $n = 10$ per group; Fig. 3D, F). Accordingly, functional attenuation of TROY in OPCs cocultured with DRG neurons increases the myelination competence of oligodendrocytes in vitro, suggesting that TROY inhibition facilitates CNS myelination.

PKC signaling has been implicated in the regulation of oligodendrocyte differentiation although its exact role in this process remains controversial [17–21]. To define the involvement of PKC in the inhibitory effects of TROY that is

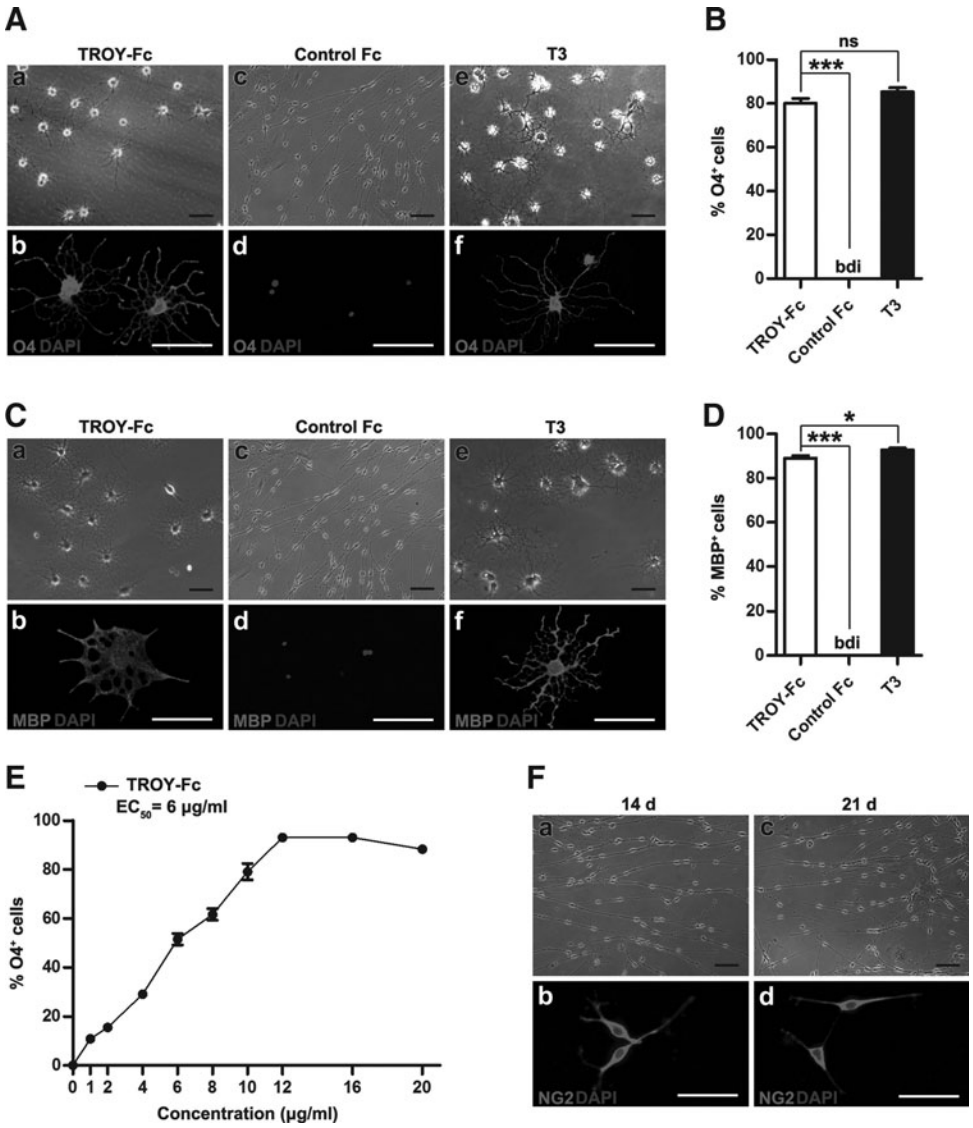

FIG. 2. TROY is involved in the negative regulation of OPC differentiation. **(A)** Primary OPC cultures treated with TROY-Fc or control Fc for 14 days. **(a)** Phase-contrast image of culture treated with TROY-Fc. **(b)** Immunofluorescence image of a representative culture treated with TROY-Fc and stained for O4 and counterstained by DAPI. **(c)** Phase-contrast image of a culture treated with control Fc. **(d)** Immunofluorescence image of a culture treated with control Fc and stained for O4 and counterstained by DAPI. **(e)** Phase-contrast image of culture treated with T3. **(f)** Immunofluorescence image of a representative culture treated with T3 and stained for O4 and counterstained by DAPI. **(B)** Quantitative analysis of percentage of O4-positive cells in OPC cultures treated with TROY-Fc, control Fc, or T3 for 14 days. Data are presented as mean ± SEM; bdi, below detectable limit; ***$P < 0.001$; ns, nonsignificant; $n = 10$ per group. **(C)** Primary OPC cultures treated with TROY-Fc or control Fc for 21 days. **(a)** Phase-contrast image of culture treated with TROY-Fc. **(b)** Immunofluorescence image of culture treated with TROY-Fc and stained for MBP and counterstained by DAPI. **(c)** Phase-contrast image of culture treated with control Fc. **(d)** Immunofluorescence image of culture treated with control Fc and stained for MBP and counterstained by DAPI. **(e)** Phase-contrast image of culture treated with T3. **(f)** Immunofluorescence image of a representative culture treated with T3 and stained for MBP and counterstained by DAPI. **(D)** Quantitative analysis of percentage of MBP-positive cells in OPC cultures treated with TROY-Fc, control Fc, or T3 for 21 days. Data are presented as mean ± SEM; bdi, below detectable limit; *$P < 0.05$; ***$P < 0.001$; ns, nonsignificant; $n = 10$ per group. **(E)** Quantitative analysis of dose-dependent effects of TROY-Fc on oligodendrocyte differentiation after 14-day treatment. Data are presented as mean ± SEM; EC_{50}, half-maximum effective concentration; $n = 5$ per concentration. **(F)** Primary OPC cultures treated with TROY-Fc or control Fc for 14 days or 21 days. **(a)** Phase-contrast image of culture treated with control Fc for 14 days. **(b)** Immunofluorescence image of a representative culture treated with control Fc for 14 days and stained for NG2 and counterstained by DAPI. **(c)** Phase-contrast image of a culture treated with control Fc for 21 days. **(d)** Immunofluorescence image of a culture treated with control Fc for 21 days and stained for NG2 and counterstained by DAPI. Scale bars: **(A-a, A-e, C-a, C-e)** = 200 µm; **(A-b, A-f, C-b, C-f, F-a, F-b)** = 50 µm; **(A-c, A-d, C-c, C-d, F-a, F-c)** = 100 µm. EC_{50}, half-maximum effective concentration; SEM, standard error of the mean; T3, triiodo-L-thyronine; TROY-Fc, soluble human TROY.

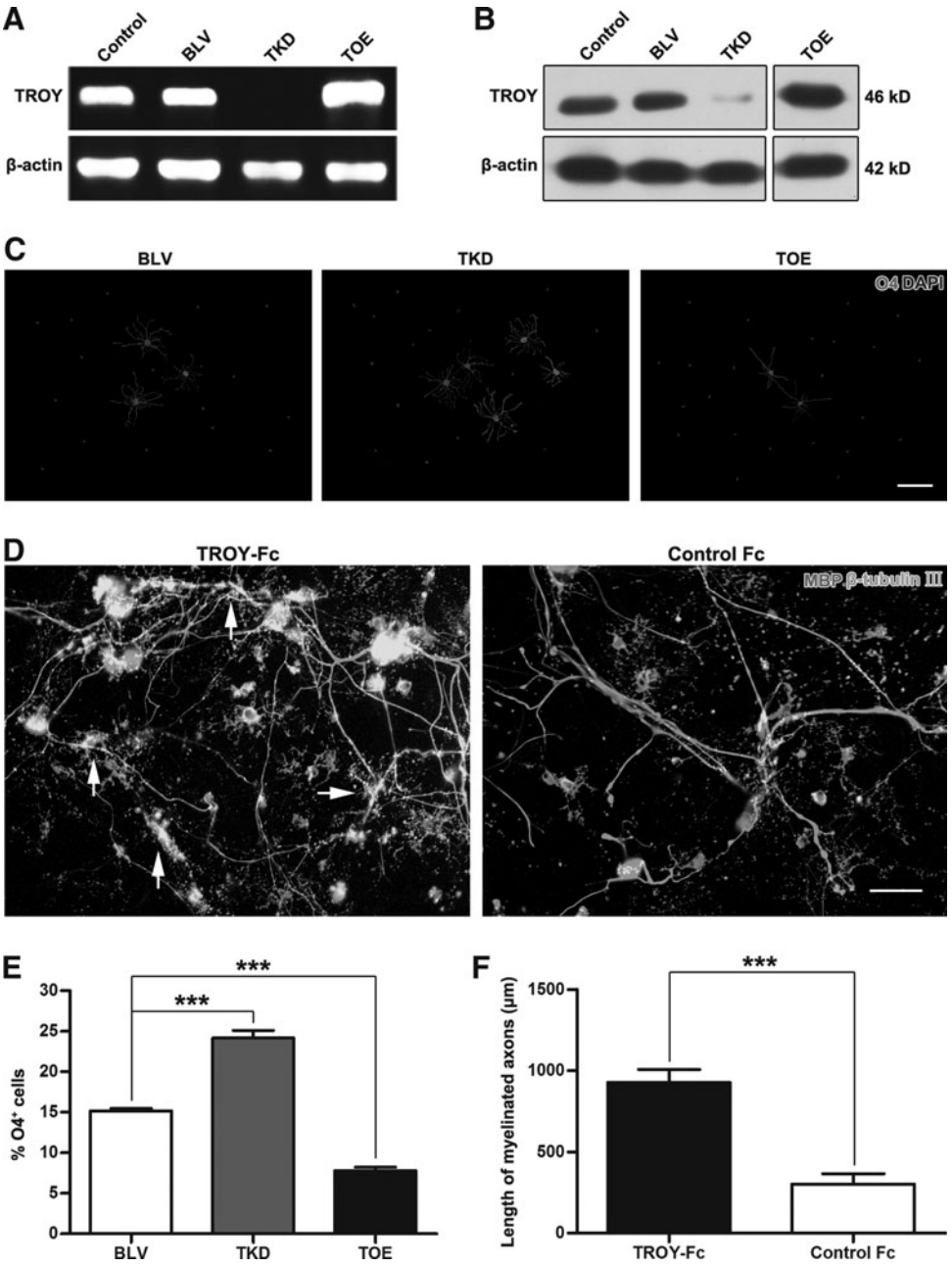

FIG. 3. TROY inhibition contributes to the maturation and myelination of oligodendrocytes. **(A)** Images of RT-PCR analysis of *TROY* transcription in OPCs treated with *TROY* RNAi-lentiviral vector or *TROY* lentiviral expression vector. β-Actin expression was analyzed as an internal control. **(B)** Images of western blot analysis of TROY expression in OPCs treated with *TROY* RNAi-lentiviral vector or *TROY* lentiviral expression vector. β-Actin expression was analyzed as an internal control. **(C)** Fluorescence images of TKD or TOE-OPC cultures stained for O4 and counterstained by DAPI. **(D)** Fluorescence images of TROY-Fc- or control Fc-treated OPC and DRG neuron coculture stained for β-tubulin III and MBP and counterstained by DAPI. *Arrows* denote the myelinated axons identified as the colocalization of MBP-positive oligodendrocyte processes and β-tubulin-III-positive neuritis. **(E)** Quantitative analysis of O4-positive cells in TKD or TOE-OPC cultures. Data are presented as mean ± SEM; $***P < 0.001$; $n = 5$ per group. **(F)** Quantitative analysis of length of myelinated axons in TROY-Fc- or control Fc-treated OPC and DRG neuron cocultures. Data are presented as mean ± SD; $***P < 0.001$; $n = 10$ per group. Scale bars: **(C)** = 50 μm; **(D)** = 25 μm. BLV, blank lentiviral vector; DRG, dorsal root ganglion; PKC, protein kinase C; RNAi, RNA interference; SD, standard deviation; TKD, *TROY* knockdown; TOE, TROY overexpression.

demonstrated to function through c-Jun terminal kinase (c-JNK), the levels of c-JNK and phosphorylated PKC (p-PKC) were measured by western blot assays. As shown in Fig. 4A and C–E, in TROY-overexpressing OPCs with differentiation inhibition, the expression of c-JNK ($F = 110.5$; TOE, $P < 0.001$ versus BLV; $n = 5$ per group) and the activation of PKC were notably enhanced ($F = 479.2$; TOE, $P < 0.001$ versus BLV; $n = 5$ per group). In contrast, the *TROY*-knockdown (TKD) OPCs with augmented differentiation potential displayed relatively reduced c-JNK ($F = 110.5$; TKD, $P < 0.001$ versus BLV; $n = 5$ per group) and p-PKC levels ($F = 479.2$; TKD, $P < 0.001$ versus BLV; $n = 5$ per group). To further determine whether PKC transduction is implicated in the TROY-mediated OPC differentiation arrest, the pharmacological inhibitor of PKC (BIM) was added to the OPC culture in absence or presence of TROY overexpression. As shown in Fig. 4A and F, mere PKC inhibitor supplement (PKC inhibition, PKCi) was capable of slightly but significantly increasing the expression of MBP in OPC culture differentiated for 7 days ($F = 63.95$; BLV + PKCi, $P < 0.05$ versus BLV; $n = 5$ per group). Further, although overexpression of TROY resulted in an evident decrease in MBP level in differentiated oligodendrocytes ($F = 63.95$; TOE, $P < 0.001$ versus BLV; $n = 5$ per group), functional attenuation of PKC obviously rescued the MBP expression ($F = 63.95$; TOE + PKCi, $P < 0.001$ versus TOE; $n = 5$ per group). However, the level of MBP in cultures treated with the *TROY* lentiviral expression vector and PKC inhibitor

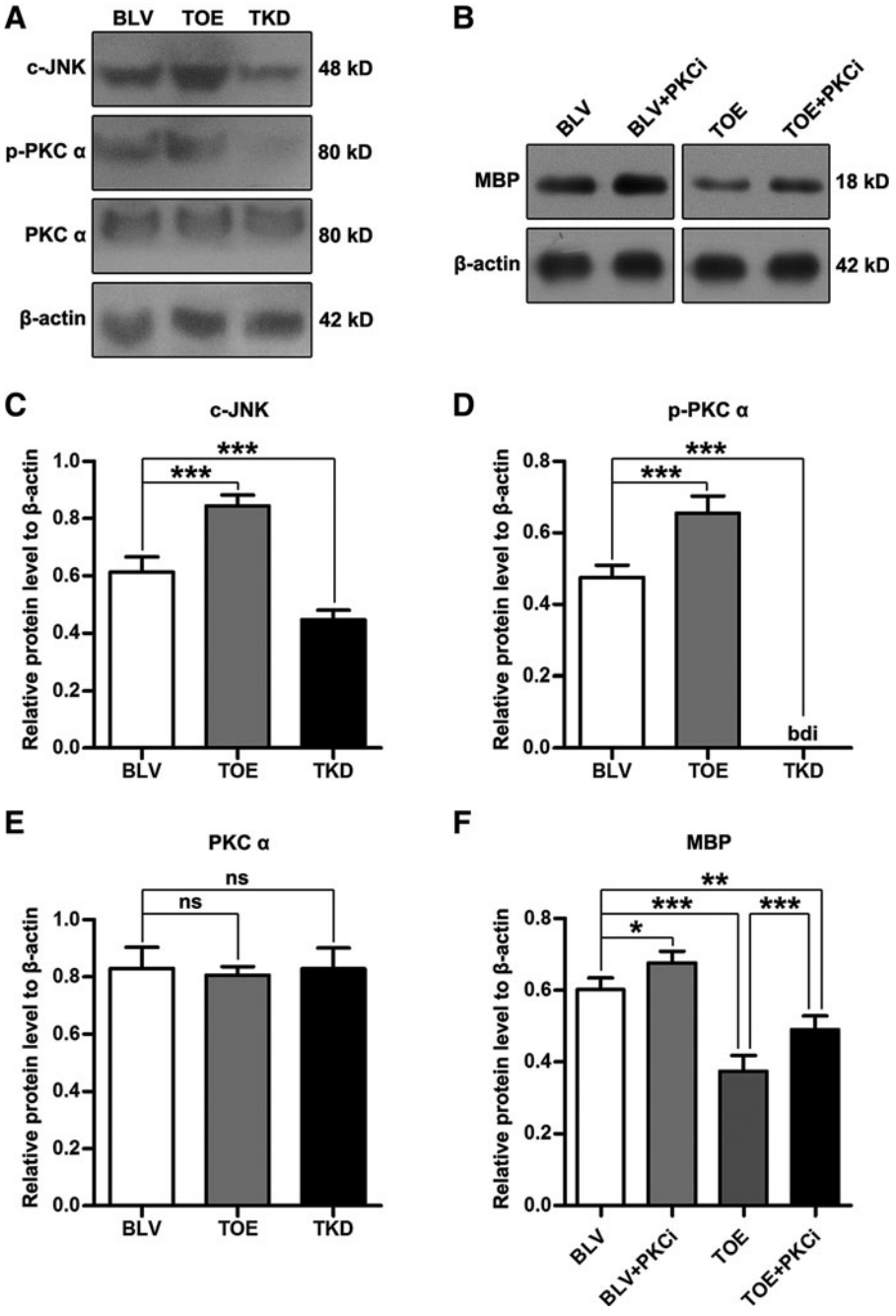

FIG. 4. Inhibitory effects of TROY are at least partly mediated by PKC signaling. **(A)** Images of western blot analysis of c-JNK, p-PKC-α, and PKC-α expression in OPC cultures treated with *TROY* RNAi-lentiviral vector or *TROY* lentiviral expression vector. β-Actin expression was analyzed as an internal control. **(B)** Images of western blot analysis of MBP expression in OPC cultures treated with BLV, BLV plus PKC inhibitor, *TROY* lentiviral expression vector, or TROY lentiviral expression vector plus PKC inhibitor. β-Actin expression was analyzed as an internal control. **(C–E)** Quantitative analysis of c-JNK, p-PKC-α, and PKC-α expression in OPC cultures treated with *TROY* RNAi-lentiviral vector or *TROY* lentiviral expression vector. Data are presented as mean ± SD; $***P < 0.001$; ns, nonsignificant; $n = 5$ per group. **(F)** Quantitative analysis of MBP expression in OPC cultures treated with BLV, BLV plus PKC inhibitor, *TROY* lentiviral expression vector, or *TROY* lentiviral expression vector plus PKC inhibitor. Data are presented as mean ± SD; $*P < 0.05$; $**P < 0.01$; $***P < 0.001$; ns, nonsignificant; $n = 5$ per group. c-JNK, c-Jun N-terminal kinase; PKCi, protein kinase C inhibition; p-PKC, phosphorylated protein kinase C.

was not raised up to that in cells treated with the BLV ($F = 63.95$; TOE + PKCi, $P < 0.001$ versus TOE, $P < 0.01$ versus BLV; $n = 5$ per group). These results suggested that the inhibitory effects of TROY on OPC maturation are mediated, at least partly, by PKC signaling transduction.

TROY inhibition reinforces the morphological restoration by OPC graft in rats with SCI

Since the in vitro effects of TROY on the differentiation of OPCs were verified, the impact of the molecule on the repair potential of grafted OPCs for SCI was further investigated in vivo through the grafting of TKD-OPCs in the rats with SCI. HE-stained axial paraffin sections of spinal cord exhibited evident cavitation and tissue loss at the epicenter of the lesion, indicative of the successive induction of SCI (Fig. 5A). After SCI rats received OPC graft for 21 days, HE staining on sagittal paraffin sections showed better recovery of spinal cord tractus in TKD-OPC-treated rats in contrast to the BLV-OPC-treated group (Fig. 5B). Immunohistochemical staining confirmed the survival of transplanted cells for at least 21 days (Fig. 5C). Although no significant difference existed in the survival of grafted cells ($t = 0.08684$; TKD-OPC, $P > 0.05$ versus BLV-OPC; Fig. 5C, D), notably more MBP^+/GFP^+ cells were detected in the lesion sites of the spinal cord of TKD-OPC-grafted rats when compared with BLV-OPC-grafted animals ($t = 5.787$; TKD-OPC, $P < 0.001$ versus BLV-OPC; Fig. 5C, E), suggesting that TKD promotes the differentiation of grafted OPCs in the host spinal cord tissue. To further investigate the remyelination post-SCI, LFB staining and ultramicropathological analysis were performed. As shown by LFB staining (Fig. 6A), evident demyelination was clearly observed at lesion sites one week after SCI. Consistent with enhanced OPC differentiation and accelerated remyelination, overall myelinated area increased evidently at lesion sites at week 3 following OPC grafting (ie, 4 weeks post-SCI) in contrast to that observed in animals received BLV-OPC grafting ($F = n$; TKD-OPC, $P < 0.01$ versus BLV-OPC; $n = 6$ per group; Fig. 6A, C). Early after the injury, the

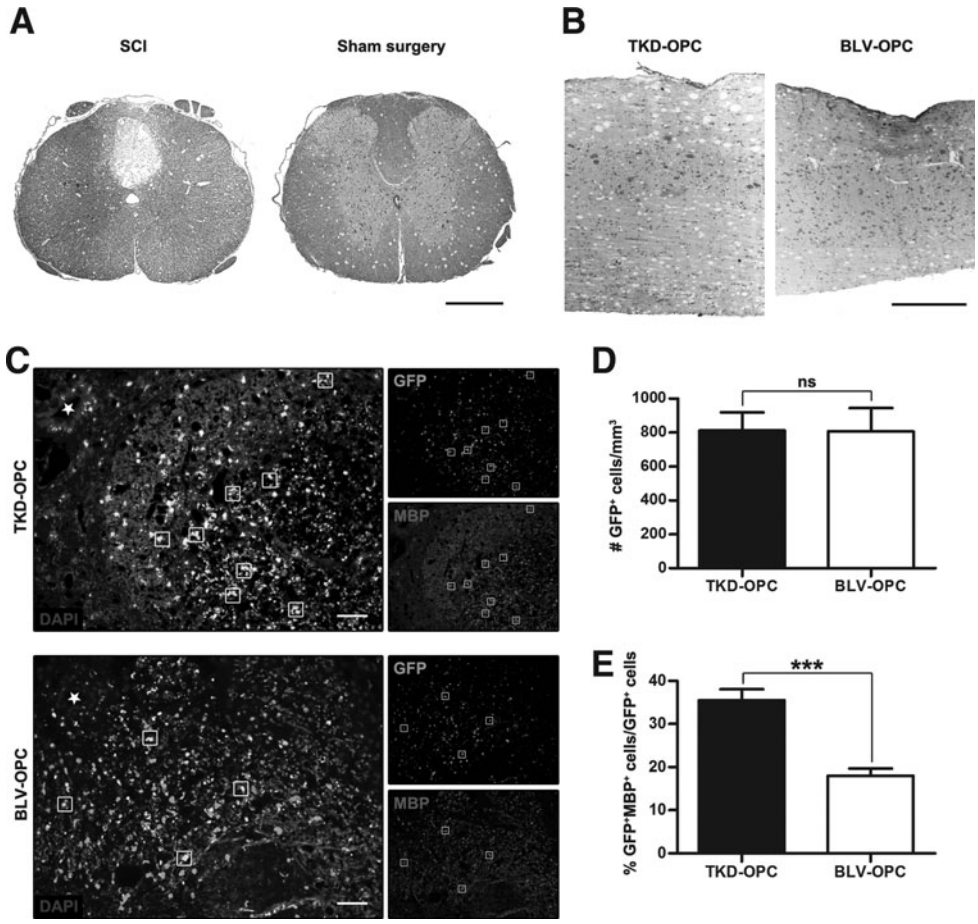

FIG. 5. TROY inhibition reinforces maturation of grafted OPCs in rats with SCI. **(A)** Images of HE-stained axial sections at the lesion epicenter of spinal cord. **(B)** Images of HE-stained sagittal sections at the lesion epicenter 28 days following SCI (21 days after grafting). **(C)** Immunofluorescence images of axial sections at the lesion epicenter 28 days following SCI (21 days after grafting). Square frames denote the GFP and MBP double-positive graft-derived mature oligodendrocyte. Pentagram denotes central canal of spinal cord. **(D)** Quantitative analysis of GFP-positive grafted cells in host spinal cord tissue. Data are presented as mean ± SEM; ns, nonsignificant; $n = 6$ per group. **(E)** Quantitative analysis of percentage of GFP and MBP double-positive graft-derived mature oligodendrocyte in host spinal cord tissue. Data are presented as mean ± SEM; *** $P < 0.001$; $n = 6$ per group. Scale bars: **(A** and **B)** = 500 μm; **(C)** = 100 μm. GFP, green fluorescent protein; HE, hematoxylin-eosin; SCI, spinal cord injury.

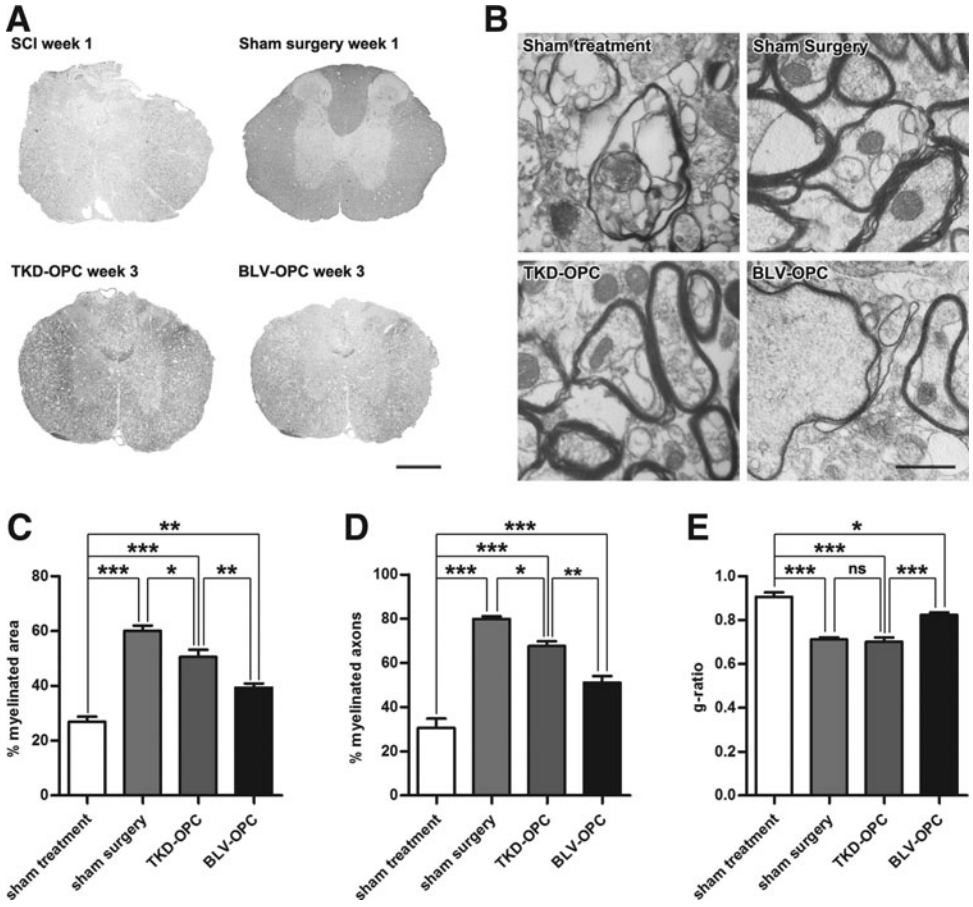

FIG. 6. TROY inhibition reinforces remyelination by OPC graft in rats with SCI. **(A)** Images of LFB-stained axial sections at the lesion epicenter 1 week following SCI or 3 weeks following grafting (4 weeks following SCI). **(B)** TEM images of axial sections at the lesion epicenter 28 days following SCI (21 days after grafting). **(C)** Quantitative analysis of proportion of LFB-stained myelinated area at the lesion epicenter 4 weeks following SCI. **(D)** Quantitative analysis of percentage of myelinated axons at the lesion epicenter 4 weeks following SCI. **(E)** Quantitative analysis of g-ratio of myelinated axons at the lesion epicenter 4 weeks following SCI. For **(C)**, **(D)**, and **(E)**, data are presented as mean ± SEM; $*P < 0.05$; $**P < 0.01$; $***P < 0.001$; $n = 6$ per group. Scale bars: **(A)** = 500 μm; **(B)** = 1 μm. LFB, Luxol fast blue; TEM, transmission electron microscope.

myelin regenerated by oligodendrocytes forms shorter and more thinly packed sheaths surrounding axons, in contrast to the surviving native myelin that features densely packed layers wrapping the axon. This difference in length and thickness around axons has been selected as an indicator of remyelination following injury by grafted or endogenous cells [38,39]. In the present study, the ultramicrohistological analyses revealed that the rats that received TKD-OPC grafting for 21 days were detected with more newly generated thinly packed myelin sheaths that could be simply distinguished from native uninjured dense myelins. In comparison, rats subjected to BLV-OPC graft showed less remyelination after transplantation, whereas rats sham-treated with PBS displayed only primarily disrupted or damaged myelin sheaths and very little remyelination (Fig. 3D). Additionally, quantitative analyses further revealed that the TKD-OPC-grafted rats had significantly higher percentage of preserved myelinated axons ($F = 56.87$; TKD-OPC, $P < 0.001$ versus sham treatment, $P < 0.01$ versus BLV-OPC; $n = 6$ per group) and lower g-ratio (ratio of axon diameter to myelinated axon diameter; $F = 34.54$; TKD-OPC, $P < 0.001$ versus sham treatment, $P < 0.001$ versus BLV-OPC; $n = 6$ per group) in comparison with BLV-OPC-grafted animals, which even statistically demonstrated the remarkable remyelination competence of TKD-OPCs. Thus, the results of these morphological analyses, consistent with each other, verified the positive effects of TROY inhibition on the repair potential of OPCs for SCI.

TROY inhibition intensifies the functional recovery by grafting of OPCs in SCI rats

BBB assessment, which involves the examination of hindlimb motor function, was performed to evaluate the impact of TROY inhibition on the therapeutic efficacy of OPCs. As shown in Fig. 7A, a clear functional defect was detected in rats at day 1 following SCI in comparison with those in the sham surgery group (TKD-OPC, BLV-OPC, and sham treatment, $P < 0.001$ versus sham surgery group on day 1 following SCI; $n = 6$ per group), verifying the successful induction of SCI. Although rats with SCI displayed a gradual improvement in motor function over time ($F_{time} = 1{,}924$, $P < 0.001$, $n = 6$ per group per time point), no difference was detected before grafting (7 days following SCI) between the treatment groups and the sham treatment group ($F_{group} = 5{,}614$; TKD-OPC and BLV-OPC, $P > 0.05$ versus sham treatment on days 1, 3, and 7 following SCI; $n = 6$ per group per time point). From 3 days after the transplantation treatment (10 days following SCI) to the end of observation (28 days following SCI), rats in the treatment groups attained higher scores than those in the sham treatment group (TKD-OPC and BLV-OPC, $P < 0.001$ versus sham treatment on 10, 14, 17, 21, 24, and 28 days following SCI; $n = 6$ per group per time point), indicative of the effectiveness of OPC graft treatment for SCI. However, rats receiving grafting of TKD-OPCs displayed better recovery than those undergoing transplantation of BLV-treated OPCs since a week after

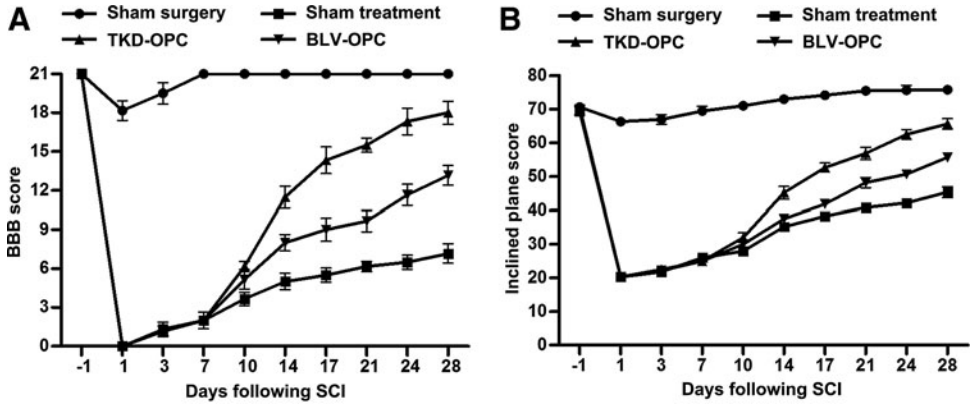

FIG. 7. TROY inhibition intensifies motor function recovery by grafting of OPCs in SCI rats. **(A)** Quantitative analysis of BBB scores of rats. Transplantation was performed on day 7 following SCI. Data are presented as mean ± SD; $n = 6$ per group per time point. **(B)** Quantitative analysis of inclined plane score of rats on the inclined plane. Transplantation was performed on day 7 following SCI. Data are presented as mean ± SD; $n = 6$ per group per time point.

grafting (14 days following SCI) (TKD-OPC, $P < 0.001$ versus BLV-OPC on days 14, 17, 21, 24, and 28 following SCI; $n = 6$ per group per time point). At the end of observation, TKD-OPC-grafted rats scored 18 ± 0.89, indicative of nearly normal movement except for asynergic tail and instable trunk. In contrast, BLV-OPC-grafted rats achieved merely a score of 13 ± 0.75, indicating frequent to consistent weight supported plantar steps and frequent forelimb–hindlimb coordination. These data suggest an enhanced therapeutic efficacy of TKD-OPCs. Inclined plane test was employed as another index to assess hindlimb strength restoration (Fig. 7B). Consistent with outcomes of BBB assessment, the data from the inclined plane test showed an effective SCI induction on rats ($F_{group} = 8{,}261$; TKD-OPC, BLV-OPC, and sham treatment, $P < 0.001$ versus sham surgery group on day 1 following SCI; $n = 6$ per group) and a time-dependent recovery of motor function of SCI rats ($F_{time} = 3{,}295$; $P < 0.001$; $n = 6$ per group per time point). The inclined plane test also showed that although OPC grafting contributed to functional recovery (TKD-OPC, $P < 0.001$ versus sham treatment on days 10, 14, 17, 21, 24, and 28 following SCI; BLV-OPCs, $P < 0.05$ versus sham treatment on day 10 following SCI, $P < 0.01$ versus sham treatment on day 14 following SCI, $P < 0.001$ versus sham treatment on 17, 21, 24, and 28 days following SCI; $n = 6$ per group per time point), the restoration of motor function in rat receiving TKD-OPC graft was augmented (TKD-OPC, $P < 0.05$ versus BLV-OPC on day 10 following SCI, $P < 0.001$ versus BLV-OPC on days 10, 14, 17, 21, 24, and 28 following SCI; $n = 6$ per group per time point). These data demonstrate that TKD improves the therapeutic efficacy of OPCs after SCI.

MEP has been widely used in clinical and animal trials of SCI to evaluate neuromuscular system function. In the present study, the latency of MEP was used to assess motor function objectively (Fig. 8A, C). At week 1 after injury, waves could not be detected in all rats that underwent the SCI induction surgery. However, at week 3 after grafting (week 4 after injury), grafted rats exhibited MEP waves compared with the sham-treated animals in which waves were still undetectable. Further, the latency of TKD-OPC-grafted rats (2.10 ± 0.13 ms) became comparable to that of the sham surgery rats (2.08 ± 0.15 ms), whereas that of BLV-treated cell-grafted rats (3.60 ± 0.19 ms) was significantly longer ($F = 713$; TKD-OPC, $P > 0.05$ versus sham surgery; $P < 0.001$ versus BLV-OPC; $n = 6$ per group). To further determine the impairment and restoration of nerve conduction tractus, another electrophysiological analysis, SEP analysis, was performed (Fig. 8A, D). Similar to MEP, SEP is virtually absent at week 1 following SCI in animals of all groups except sham surgery group. Sham-treatment rats show little-to-no recovery thereafter up to 28 days following injury, whereas week 4 after injury (week 3 after grafting), animals in cell-grafted groups were detected with evident waves and TKD cell-grafted rats were determined with evidently faster conduction of SEP (16.5 ± 0.55 ms) in contrast to BLV-treated cell-grafted rats (18.03 ± 0.18 ms) ($F = 3{,}683$; TKD-OPC, $P < 0.001$ versus BLV-OPC; $n = 6$ per group). Inconsistent with the results of MEP analysis, at the end of observation (week 4 after injury, ie, week 3 after grafting), SEP conduction in TKD-OPC-grafted rats was still slower than that of sham surgery rats (14.93 ± 0.34 ms) (TKD-OPC, $P < 0.001$ versus sham surgery; $n = 6$ per group).

Collectively, the validity of promoting effects of TROY inhibition on therapeutic efficacy of OPCs for SCI was demonstrated by the data of behavioral and electrophysiological assays that are consistent and confirmed each other.

Discussion

TROY serves important regulatory roles in neuronal and glial cell development in CNS and olfactory system [22–25]. Besides, it is also demonstrated to mediate caspase-independent cell death [40,41], regulate neuronal regeneration and axonal outgrowth [26,27], modulate glial-neuronal interactions in demyelination lesions [42], and even promote glioblastoma cell invasion [43,44]. In this study, we demonstrate that TROY is involved in the modulation of oligodendrocyte lineage maturation and remyelination of injured spinal cord by graft-derived oligodendrocytes.

Strikingly, the expression of TROY was detected by RT-PCR and western blot analysis in oligodendrocytes at different stages of differentiation (Fig. 1B, C), which suggest the possibility of TROY function in oligodendrocyte

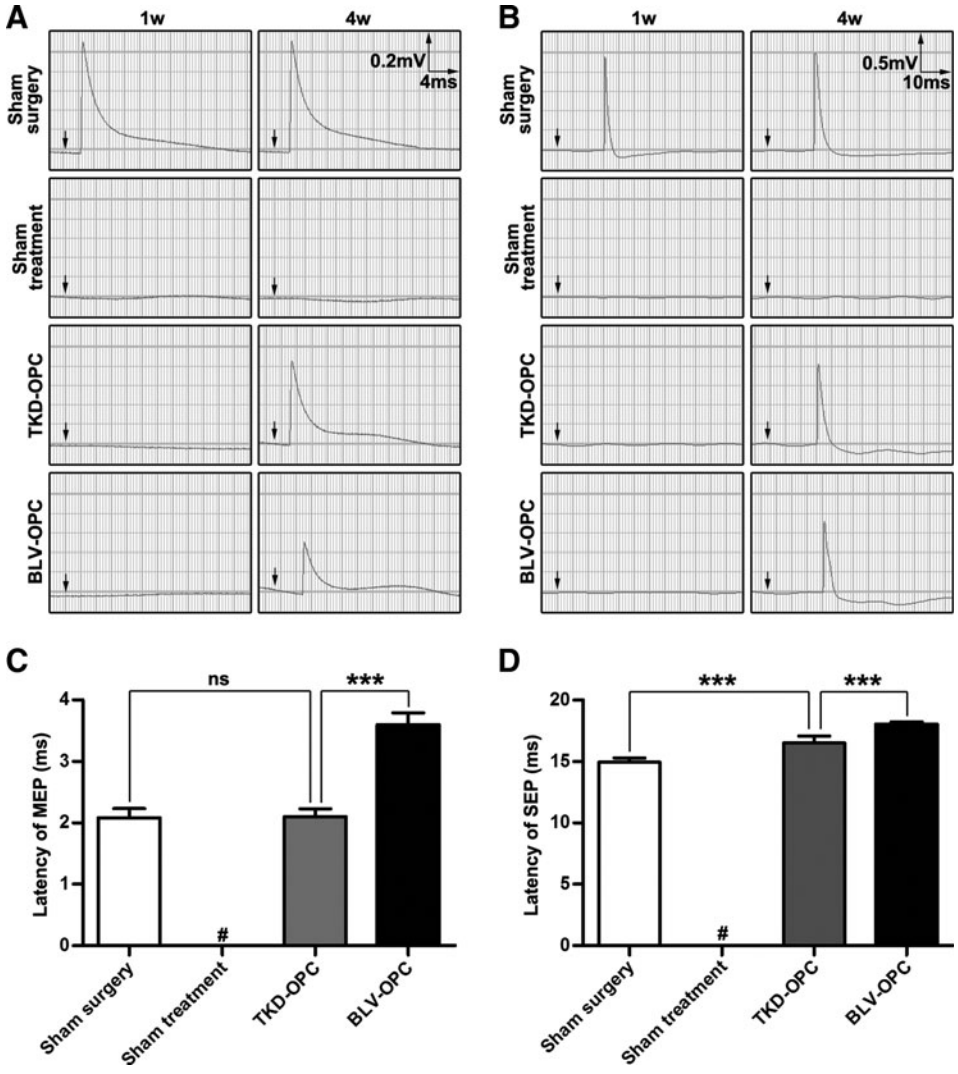

FIG. 8. TROY inhibition intensifies nerve conduction tractus recovery by grafting of OPCs in SCI rats. **(A)** Representative profiles of MEPs recorded at week 1 and week 4 after injury. Calibration bar denotes 0.2 mV/4 ms. *Arrow* indicates stimulus. **(B)** Representative profiles of SEPs recorded at week 1 and week 4 after injury. Calibration bar denotes 0.5 mV/10 ms. *Arrow* indicates stimulus. **(C)** Quantitative analysis of latency of MEP measured at week 4 after injury (week 3 after grafting). Data are presented as mean ± SD. ns, nonsignificant; $***P <$ 0.001. #, waves were not detected in sham treatment group. $n = 6$ per group. **(D)** Quantitative analysis of latency of SEP measured at week 4 after injury (week 3 after grafting). Data are presented as mean ± SD. $***P < 0.001$. #, waves were not detected in sham treatment group. $n = 6$ per group. MEP, motor-evoked potential; SEP, somatosensory evoked potential.

lineage. Following which, efforts were made to test the TROY effect on OPC differentiation. To exclude the possible impacts of other factors, the differentiation assays were performed in DMEM/F-12 supplemented only by TROY-Fc, which serves as the competitive antagonist of TROY [26]. The results verified the inhibitory effects of TROY on oligodendrocyte differentiation (Fig. 2A–E), which was further confirmed by the differentiation status of TKD-OPCs and TOE-OPCs (Fig. 3C, E). Of note, although TROY expression in various differentiation stages of oligodendrocyte lineage was determined (Fig. 1B, C), OPCs with silenced *TROY* remained capable of maturation (Figs. 3C and 4B), indicating that TROY is probably dispensable in physiological development of oligodendrocyte and the inhibitory effects of TROY may mainly function in pathophysiological process, such as demyelination and remyelination. However, the specific mechanism remains to be determined. Coinciding with the results of the differentiation assay, pharmacological inhibition of TROY resulted in the development of MBP^+ myelin-like structures surrounding axons in cocultures of OPCs and DRG neurons (Fig. 3D). To date, coculture with isolated DRG neurons tends to be considered as the standard method to measure the myelin-sheath-forming capability of OPCs and Schwann cells in vitro [13,30,37]. The distinction in the in vitro myelination competence of OPCs between in presence and absence of TROY-Fc further confirmed the negative effects of TROY upon CNS myelination.

To further elucidate the molecular mechanism underlying the inhibitory effects of TROY on oligodendrocyte development, the signaling pathways mediating OPC differentiation should be tested. Previous studies implicate PKC signaling transduction in the oligodendrocyte differentiation inhibition [17,18,20], particularly in the demyelination-derived myelin debris-induced OPC differentiation block [19]; however, the opposing opinion also exists that PKC promotes the expression of MBP by phosphorylating transcription factor Sp1 [21]. Further, c-JNK pathway through which TROY mediates caspase-independent cell death is also modulated by PKC signaling [40,45–47]. Our data showed that the oligodendrocyte differentiation progression inversely correlated with the activity of PKC and PKC-regulated c-JNK signaling and the pharmacological inhibition of PKC reversed the inhibitory effects of TROY overexpression on OPC differentiation (Fig. 4). These results verified the involvement of PKC in the negative regulation of oligodendrocyte maturation mediated by TROY. These findings may shed light on the strategies promoting the oligodendrocyte maturation and remyelination.

In SCI, which is characterized by major damage to neurons and myelin sheaths, remyelination failure results in disruption of normal nerve conduction and delay of functional recovery [7,8]. OPC grafts contribute to remyelination and therefore aid in restoring normal conduction [5,38,48]. However, OPC graft therapy faces two main challenges, one of which is the lack of abundant purified cell source. OPCs only constitute 5% of total cells in adult brain and the primary OPCs are not readily available [1,49]. Moreover, the derivation of engraftable OPCs from pluripotent stem cells, including embryonic stem cells and induced pluripotent stem cells, has proven slow and tedious [49–52]. Accordingly, effective in vitro expansion of OPCs is essential for successful graft treatment. The discovery that PDGF is required for the survival and proliferation of OPCs led to the identification of PDGFRA as a determinant marker of OPCs [1]. Inconsistently, we obtained purified and highly proliferative OPC culture using DMEM/F-12 supplemented with FBS instead of bFGF and PDGF (Fig. 1A), which may suggest the existence of PDGF mimics in complex FBS and lead to the development of more convenient methods for the culture and expansion of OPCs. The other challenge is the microenvironment in the lesion sites dampening the differentiation and remyelination of OPCs [7,8]. Hence, an effective strategy that promotes the maturation of grafted cells is required for successful OPC transplantation and remyelination. In accordance with in vitro findings that indicate that the functional repression of TROY facilitated OPC differentiation and augmented the myelination competence, TKD significantly improved the repair potential of grafted OPCs for SCI. TKD-OPCs that survived and developed into mature MBP^+ myelinating cells at lesion epicenters brought about evident remyelination and morphological restoration (Figs. 5 and 6). In parallel, animals that received TKD-OPC graft showed notable recovery in motor and nerve conduction tractus function (Figs. 7 and 8). These findings provide evidence that supports effects of TROY inhibition on oligodendrocyte development and the therapeutic efficacy of OPC graft on SCI.

Summary

In summary, TROY (tumor necrosis factor receptor superfamily member 19), which is expressed in the oligodendrocyte lineage on various differentiation stages, serves as an important negative regulator of OPC differentiation and myelination. Further, silencing of TROY expression in grafted OPCs significantly improves the therapeutic efficacy for SCI, resulting in evident morphological and neurological recovery. Our research identifies TROY as a new modulator in oligodendrial maturation and a new target in enhancing remyelination after CNS injury.

Acknowledgments

The authors thank Xinlei Li and Jingbo Zhang for their outstanding technical support. This work was supported by the grants from the National Natural Science Foundation of China (81073162; to S.W.), the Science Foundation for the Returned Overseas Students for Heilongjiang Province (Lc201016; to S.W.), and the Heilongjiang Province Office of Education (11551181; to S.W.).

Author Disclosure Statement

The authors indicate no potential conflicts of interest.

References

1. Nishiyama A, M Komitova, R Suzuki and X Zhu. (2009). Polydendrocytes (NG2 cells): multifunctional cells with lineage plasticity. Nat Rev Neurosci 10:9–22.
2. Vigano F, W Mobius, M Gotz and L Dimou. (2013). Transplantation reveals regional differences in oligodendrocyte differentiation in the adult brain. Nat Neurosci 16:1370–1372.
3. Hughes EG, SH Kang, M Fukaya and DE Bergles. (2013). Oligodendrocyte progenitors balance growth with self-repulsion to achieve homeostasis in the adult brain. Nat Neurosci 16:668–676.
4. Yu Y, Y Chen, B Kim, H Wang, C Zhao, X He, L Liu, W Liu, LM Wu, et al. (2013). Olig2 targets chromatin remodelers to enhancers to initiate oligodendrocyte differentiation. Cell 152:248–261.
5. Waxman SG. (2006). Axonal conduction and injury in multiple sclerosis: the role of sodium channels. Nat Rev Neurosci 7:932–941.
6. Courtine G, MB Bunge, JW Fawcett, RG Grossman, JH Kaas, R Lemon, I Maier, J Martin, RJ Nudo, et al. (2007). Can experiments in nonhuman primates expedite the translation of treatments for spinal cord injury in humans? Nat Med 13:561–566.
7. Imai M, M Watanabe, K Suyama, T Osada, D Sakai, H Kawada, M Matsumae and J Mochida. (2008). Delayed accumulation of activated macrophages and inhibition of remyelination after spinal cord injury in an adult rodent model. J Neurosurg Spine 8:58–66.
8. Su Z, Y Yuan, J Chen, Y Zhu, Y Qiu, F Zhu, A Huang and C He. (2011). Reactive astrocytes inhibit the survival and differentiation of oligodendrocyte precursor cells by secreted TNF-alpha. J Neurotrauma 28:1089–1100.
9. Meijer DH, MF Kane, S Mehta, H Liu, E Harrington, CM Taylor, CD Stiles and DH Rowitch. (2012). Separated at birth? The functional and molecular divergence of OLIG1 and OLIG2. Nat Rev Neurosci 13:819–831.
10. Wake H, PR Lee and RD Fields. (2011). Control of local protein synthesis and initial events in myelination by action potentials. Science 333:1647–1651.
11. Miron VE, A Boyd, JW Zhao, TJ Yuen, JM Ruckh, JL Shadrach, P van Wijngaarden, AJ Wagers, A Williams, RJ Franklin and C Ffrench-Constant. (2013). M2 microglia and macrophages drive oligodendrocyte differentiation during CNS remyelination. Nat Neurosci 16:1211–1218.
12. Furusho M, Y Kaga, A Ishii, JM Hebert and R Bansal. (2011). Fibroblast growth factor signaling is required for the generation of oligodendrocyte progenitors from the embryonic forebrain. J Neurosci 31:5055–5066.
13. Chan JR, TA Watkins, JM Cosgaya, C Zhang, L Chen, LF Reichardt, EM Shooter and BA Barres. (2004). NGF controls axonal receptivity to myelination by Schwann cells or oligodendrocytes. Neuron 43:183–191.
14. Wang S, AD Sdrulla, G diSibio, G Bush, D Nofziger, C Hicks, G Weinmaster and BA Barres. (1998). Notch receptor activation inhibits oligodendrocyte differentiation. Neuron 21:63–75.
15. Michailov GV, MW Sereda, BG Brinkmann, TM Fischer, B Haug, C Birchmeier, L Role, C Lai, MH Schwab and KA Nave. (2004). Axonal neuregulin-1 regulates myelin sheath thickness. Science 304:700–703.

16. Liang X, NA Draghi and MD Resh. (2004). Signaling from integrins to Fyn to Rho family GTPases regulates morphologic differentiation of oligodendrocytes. J Neurosci 24:7140–7149.
17. Baron W, JC de Jonge, H de Vries and D Hoekstra. (1998). Regulation of oligodendrocyte differentiation: protein kinase C activation prevents differentiation of O2A progenitor cells toward oligodendrocytes. Glia 22: 121–129.
18. Heinrich M, M Gorath and C Richter-Landsberg. (1999). Neurotrophin-3 (NT-3) modulates early differentiation of oligodendrocytes in rat brain cortical cultures. Glia 28:244–255.
19. Baer AS, YA Syed, SU Kang, D Mitteregger, R Vig, C Ffrench-Constant, RJ Franklin, F Altmann, G Lubec and MR Kotter. (2009). Myelin-mediated inhibition of oligodendrocyte precursor differentiation can be overcome by pharmacological modulation of Fyn-RhoA and protein kinase C signalling. Brain 132:465–481.
20. Paez PM, DJ Fulton, V Spreur, V Handley and AT Campagnoni. (2010). Multiple kinase pathways regulate voltage-dependent Ca2+ influx and migration in oligodendrocyte precursor cells. J Neurosci 30:6422–6433.
21. Guo L, T Eviatar-Ribak and R Miskimins. (2010). Sp1 phosphorylation is involved in myelin basic protein gene transcription. J Neurosci Res 88:3233–3242.
22. Hisaoka T, Y Morikawa, T Kitamura and E Senba. (2003). Expression of a member of tumor necrosis factor receptor superfamily, TROY, in the developing mouse brain. Brain Res Dev Brain Res 143:105–109.
23. Hisaoka T, Y Morikawa, T Komori, T Sugiyama, T Kitamura and E Senba. (2006). Characterization of TROY-expressing cells in the developing and postnatal CNS: the possible role in neuronal and glial cell development. Eur J Neurosci 23:3149–3160.
24. Hisaoka T, Y Morikawa and E Senba. (2006). Characterization of TROY/TNFRSF19/TAJ-expressing cells in the adult mouse forebrain. Brain Res 1110:81–94.
25. Morikawa Y, T Hisaoka, T Kitamura and E Senba. (2008). TROY, a novel member of the tumor necrosis factor receptor superfamily in the central nervous system. Ann N Y Acad Sci 1126:A1–A10.
26. Park JB, G Yiu, S Kaneko, J Wang, J Chang, XL He, KC Garcia and Z He. (2005). A TNF receptor family member, TROY, is a coreceptor with Nogo receptor in mediating the inhibitory activity of myelin inhibitors. Neuron 45: 345–351.
27. Shao Z, JL Browning, X Lee, ML Scott, S Shulga-Morskaya, N Allaire, G Thill, M Levesque, D Sah, et al. (2005). TAJ/TROY, an orphan TNF receptor family member, binds Nogo-66 receptor 1 and regulates axonal regeneration. Neuron 45: 353–359.
28. Kotter MR, WW Li, C Zhao and RJ Franklin. (2006). Myelin impairs CNS remyelination by inhibiting oligodendrocyte precursor cell differentiation. J Neurosci 26: 328–332.
29. Chen Y, V Balasubramaniyan, J Peng, EC Hurlock, M Tallquist, J Li and QR Lu. (2007). Isolation and culture of rat and mouse oligodendrocyte precursor cells. Nat Protoc 2:1044–1051.
30. Deshmukh VA, V Tardif, CA Lyssiotis, CC Green, B Kerman, HJ Kim, K Padmanabhan, JG Swoboda, I Ahmad, et al. (2013). A regenerative approach to the treatment of multiple sclerosis. Nature 502:327–332.
31. Basso DM, MS Beattie and JC Bresnahan. (1996). Graded histological and locomotor outcomes after spinal cord contusion using the NYU weight-drop device versus transection. Exp Neurol 139:244–256.
32. Nori S, Y Okada, A Yasuda, O Tsuji, Y Takahashi, Y Kobayashi, K Fujiyoshi, M Koike, Y Uchiyama, et al. (2011). Grafted human-induced pluripotent stem-cell-derived neurospheres promote motor functional recovery after spinal cord injury in mice. Proc Natl Acad Sci U S A 108:16825–16830.
33. Maybhate A, C Hu, FA Bazley, Q Yu, NV Thakor, CL Kerr and AH All. (2012). Potential long-term benefits of acute hypothermia after spinal cord injury: assessments with somatosensory-evoked potentials. Crit Care Med 40: 573–579.
34. Gao FB, J Apperly and M Raff. (1998). Cell-intrinsic timers and thyroid hormone regulate the probability of cell-cycle withdrawal and differentiation of oligodendrocyte precursor cells. Dev Biol 197:54–66.
35. Billon N, Y Tokumoto, D Forrest and M Raff. (2001). Role of thyroid hormone receptors in timing oligodendrocyte differentiation. Dev Biol 235:110–120.
36. Fernandez M, A Giuliani, S Pirondi, G D'Intino, L Giardino, L Aloe, R Levi-Montalcini and L Calza. (2004). Thyroid hormone administration enhances remyelination in chronic demyelinating inflammatory disease. Proc Natl Acad Sci U S A 101:16363–16368.
37. Mi S, RH Miller, X Lee, ML Scott, S Shulag-Morskaya, Z Shao, J Chang, G Thill, M Levesque, et al. (2005). LINGO-1 negatively regulates myelination by oligodendrocytes. Nat Neurosci 8:745–751.
38. Keirstead HS, G Nistor, G Bernal, M Totoiu, F Cloutier, K Sharp and O Steward. (2005). Human embryonic stem cell-derived oligodendrocyte progenitor cell transplants remyelinate and restore locomotion after spinal cord injury. J Neurosci 25:4694–4705.
39. Powers BE, DL Sellers, EA Lovelett, W Cheung, SP Aalami, N Zapertov, DO Maris and PJ Horner. (2013). Remyelination reporter reveals prolonged refinement of spontaneously regenerated myelin. Proc Natl Acad Sci U S A 110:4075–4080.
40. Eby MT, A Jasmin, A Kumar, K Sharma and PM Chaudhary. (2000). TAJ, a novel member of the tumor necrosis factor receptor family, activates the c-Jun N-terminal kinase pathway and mediates caspase-independent cell death. J Biol Chem 275:15336–15342.
41. Wang Y, X Li, L Wang, P Ding, Y Zhang, W Han and D Ma. (2004). An alternative form of paraptosis-like cell death, triggered by TAJ/TROY and enhanced by PDCD5 overexpression. J Cell Sci 117:1525–1532.
42. Satoh J, H Tabunoki, T Yamamura, K Arima and H Konno. (2007). TROY and LINGO-1 expression in astrocytes and macrophages/microglia in multiple sclerosis lesions. Neuropathol Appl Neurobiol 33:99–107.
43. Paulino VM, Z Yang, J Kloss, MJ Ennis, BA Armstrong, JC Loftus and NL Tran. (2010). TROY (TNFRSF19) is overexpressed in advanced glial tumors and promotes glioblastoma cell invasion via Pyk2-Rac1 signaling. Mol Cancer Res 8:1558–1567.
44. Jacobs VL, Y Liu and JA De Leo. (2012). Propentofylline targets TROY, a novel microglial signaling pathway. PLoS One 7:e37955.
45. Brandlin I, T Eiseler, R Salowsky and FJ Johannes. (2002). Protein kinase C(mu) regulation of the JNK pathway is

triggered via phosphoinositide-dependent kinase 1 and protein kinase C(epsilon). J Biol Chem 277:45451–45457.
46. Lopez-Bergami P, H Habelhah, A Bhoumik, W Zhang, LH Wang and Z Ronai. (2005). RACK1 mediates activation of JNK by protein kinase C [corrected]. Mol Cell 19: 309–320.
47. Lopez-Bergami P and Z Ronai. (2008). Requirements for PKC-augmented JNK activation by MKK4/7. Int J Biochem Cell Biol 40:1055–1064.
48. All AH, FA Bazley, S Gupta, N Pashai, C Hu, A Pourmorteza and C Kerr. (2012). Human embryonic stem cell-derived oligodendrocyte progenitors aid in functional recovery of sensory pathways following contusive spinal cord injury. PLoS One 7:e47645.
49. Yang N, JB Zuchero, H Ahlenius, S Marro, YH Ng, T Vierbuchen, JS Hawkins, R Geissler, BA Barres and M Wernig. (2013). Generation of oligodendroglial cells by direct lineage conversion. Nat Biotechnol 31:434–439.
50. Hu BY, JP Weick, J Yu, LX Ma, XQ Zhang, JA Thomson and SC Zhang. (2010). Neural differentiation of human induced pluripotent stem cells follows developmental principles but with variable potency. Proc Natl Acad Sci U S A 107:4335–4340.
51. Najm FJ, A Zaremba, AV Caprariello, S Nayak, EC Freundt, PC Scacheri, RH Miller and PJ Tesar. (2011). Rapid and robust generation of functional oligodendrocyte progenitor cells from epiblast stem cells. Nat Methods 8: 957–962.
52. Wang S, J Bates, X Li, S Schanz, D Chandler-Militello, C Levine, N Maherali, L Studer, K Hochedlinger, M Windrem and SA Goldman. (2013). Human iPSC-derived oligodendrocyte progenitor cells can myelinate and rescue a mouse model of congenital hypomyelination. Cell Stem Cell 12:252–264.

Address correspondence to:
Prof. Shuliang Wu
Department of Anatomy
School of Basic Medical Sciences
Harbin Medical University
No. 194, Xue Fu Road
Nan Gang District
Harbin 150081
China

E-mail: wushuliang@ems.hrbmu.edu.cn

Prof. Yafang Zhang
Department of Anatomy
School of Basic Medical Sciences
Harbin Medical University
No. 194, Xue Fu Road
Nan Gang District
Harbin 150081
China

E-mail: yafangzhang2008@hotmail.com

Dr. Yongshun Duan
The First Affiliated Hospital of Harbin Medical University
No. 23, You Zheng Street
Nan Gang District
Harbin 150001
China

E-mail: zhuzi819@sohu.com

Received for publication November 17, 2013
Accepted after revision April 21, 2014
Prepublished on Liebert Instant Online April 22, 2014